



Genetic interaction between two insulin-dependent diabetes susceptibility loci, *Idd2* and *Idd13*, in determining immunoregulatory DN T cell proportion

Roxanne Collin^{1,2} · Kathy Doyon¹ · Victor Mullins-Dansereau^{1,2} · Martin Karam^{3,4} · Geneviève Chabot-Roy¹ · Erin E. Hillhouse¹ · Alexandre Orthwein^{3,4,5} · Sylvie Lesage^{1,2} 

Received: 9 February 2018 / Accepted: 12 April 2018 / Published online: 25 April 2018
© Springer-Verlag GmbH Germany, part of Springer Nature 2018

Abstract

Several immune regulatory cell types participate in the protection against autoimmune diseases such as autoimmune diabetes. Of these immunoregulatory cells, we and others have shown that peripheral CD4[−]CD8[−] double negative (DN) T cells can induce antigen-specific immune tolerance. Particularly, we have described that diabetes-prone mice exhibit a lower number of peripheral DN T cells compared to diabetes-resistant mice. Identifying the molecular pathways that influence the size of the DN T cell pool in peripheral lymphoid organs may thus be of interest for maintaining antigen-specific immune tolerance. Hence, through immunogenetic approaches, we found that two genetic loci linked to autoimmune diabetes susceptibility, namely *Idd2* and *Idd13*, independently contribute to the partial restoration of DN T cell proportion in secondary lymphoid organs. We now extend these findings to show an interaction between the *Idd2* and *Idd13* loci in determining the number of DN T cells in secondary lymphoid organs. Using bioinformatics tools, we link potential biological pathways arising from interactions of genes encoded within the two loci. By focusing on cell cycle, we validate that both the *Idd2* and *Idd13* loci influence RAD51 expression as well as DN T cell progression through the cell cycle. Altogether, we find that genetic interactions between *Idd2* and *Idd13* loci modulate cell cycle progression, which contributes, at least in part, to defining the proportion of DN T cells in secondary lymphoid organs.

Keywords Double negative T cells · Type 1 diabetes · Transgenic mice · Cell cycle

Introduction

A prominent role in the prevention of autoimmunity has been credited to various regulatory cell subsets, including peripheral immunoregulatory CD4[−]CD8[−] double negative (DN) T cells. Indeed, DN T cells have been shown to inhibit immune responses in an antigen-specific manner (Zhang et al. 2006; Zhang et al. 2000). This has major implications since the use of DN T cells in immunotherapy should therefore lead to fewer side effects and a decreased risk of infection, which remains a major concern in the application of broad immunosuppressive regimens (Bluestone et al. 2010a). As a result, DN T cells have been studied in various disease models, revealing that DN T cells display a promising therapeutic potential in the induction of allo- and xenograft tolerance (Chen et al. 2003; Ma et al. 2008; Young et al. 2002; Zhang et al. 2000) and in the prevention of both graft-vs-host disease (He et al. 2007; McIver et al. 2008; Young et al. 2003; Young et al. 2002) and

✉ Alexandre Orthwein
alexandre.orthwein@mcgill.ca

✉ Sylvie Lesage
sylvie.lesage@umontreal.ca

¹ Division of Immunology-oncology, Maisonneuve-Rosemont Hospital, Research Center, Montréal, 5415 l'Assomption Blvd, Québec H1T 2M4, Canada

² Département de microbiologie, infectiologie et immunologie, Université de Montréal, Montréal, Québec H3C 3J7, Canada

³ Division of Experimental Medicine, McGill University, Montréal, Québec H4A 3J1, Canada

⁴ Lady Davis Institute, Jewish General Hospital, 3755 Côte Ste-Catherine, Montréal, Québec H3T 1E2, Canada

⁵ Department of Oncology, McGill University, Montréal, Québec H4A 3J1, Canada

autoimmune diabetes (Dugas et al. 2010; Duncan et al. 2010; Ford et al. 2007; Zhang et al. 2011).

Using TCR transgenic models, our work has supported the contribution of DN T cells towards immune tolerance in autoimmune diabetes (Dugas et al. 2010). Specifically, we have demonstrated that TCR transgenic DN T cell proportion is low in autoimmune diabetes-susceptible mice (Dugas et al. 2010). However, the immunoregulatory function of TCR transgenic DN T cells remains unaltered in these mice (Hillhouse et al. 2010), demonstrating that a deficiency in DN T cell number, rather than function, contributes to autoimmune diabetes susceptibility. Correspondingly, the injection of DN T cells is sufficient to reduce the incidence of autoimmune diabetes in autoimmune diabetes-susceptible mice in the TCR transgenic setting (Dugas et al. 2010). These results highlight the importance of identifying the genetic determinants controlling DN T cell number as they may reveal key molecular targets to promote DN T cell development, thereby supporting immune tolerance.

As for most autoimmune diseases, susceptibility to autoimmune diabetes is a complex genetic trait (Bluestone et al. 2010b; Concannon et al. 2009). NOD (non-obese diabetic) mice, which spontaneously develop autoimmune diabetes, have facilitated the study of genetic factors underlying autoimmune diabetes susceptibility (Anderson and Bluestone 2005; Wicker et al. 2005). To date, more than 20 *Idd* (Insulin-dependent diabetes) loci linked to diabetes predisposition have been identified in NOD mice (www.T1Dbase.org), and the concordance with human diabetes susceptibility has been demonstrated for some of these loci (Driver et al. 2011; Wicker et al. 2005). Subsequent analysis of NOD.*Idd* congenic mice has revealed *Idd* regions which are sufficient to reduce insulinitis and/or diabetes incidence (Ghosh et al. 1993; Lyons et al. 2000; McAleer et al. 1995; Serreze et al. 1994). Interestingly, we have also linked certain *Idd* regions to the regulation of DN T cell number (Collin et al. 2014; Dugas et al. 2014), where increased DN T cell number is associated with autoimmune diabetes resistance (Collin et al. 2014; Dugas et al. 2010). More specifically, using a linkage analysis approach and congenic strain validation, we have shown that DN T cell proportion in peripheral lymphoid organs is a multigenic trait and that both *Idd2* and *Idd13* loci each contribute to the partial restoration of DN T cell numbers in the spleen and lymph nodes (Collin et al. 2014; Dugas et al. 2014). These results suggest that *Idd2* and *Idd13* loci modulate diabetes development, at least in part, by influencing DN T cell number.

Idd2 and *Idd13*, located on chromosome 9 and 2, respectively, are two loci linked to autoimmune diabetes susceptibility, while *Idd2* is also linked to insulinitis (Ghosh et al. 1993; Prochazka et al. 1987; Serreze et al. 1998; Serreze et al. 1994; Wicker et al. 1995). Recently, our group has shown that, in contrast to *Idd13* (Hillhouse et al. 2016), the *Idd2* locus also

protects NOD.*H2^k* mice from diabetes development and insulinitis in the 3A9 TCR:insHEL transgenic model (Collin et al. 2014). In addition to their role in DN T cell number modulation in the non-transgenic and/or TCR transgenic setting, both *Idd2* and *Idd13* loci are thought to play a role in the selection of diabetogenic T cells (Collin et al. 2014; Dugas et al. 2014; Pearce et al. 1995; Serreze et al. 1998). Accordingly, the *Idd13* interval encodes for several candidate genes implicated in the negative selection of autoreactive T cells including the Mer tyrosine kinase (*Mertk*) gene as well as multiple apoptosis-associated genes (Liston et al. 2007; Liston et al. 2004; Serreze et al. 1998; Wallet et al. 2009; Zucchelli et al. 2005), and *Idd2* encodes for *Thy1*, *Cbl*, and *Il10ra*, all likely contributors to T cell biology (Lang and Bellgrau 2004; Prochazka et al. 1987). In addition to DN T cell numbers, the *Idd13* locus also influences the proportion of merocytic dendritic cells, another cell population associated with autoimmune diabetes susceptibility (Pelletier and Lesage 2013). Altogether, the *Idd2* and *Idd13* loci clearly play a role in autoimmune diabetes progression via different mechanisms, including the modulation of DN T cell number.

For our studies, we take advantage of a spontaneous autoimmune diabetes model, namely the 3A9 TCR:insHEL transgenic mouse model. In this model, the insHEL transgene promotes hen egg lysosyme (HEL) expression under the rat insulin promoter, thus inducing pancreatic β cell specific expression, while the 3A9 TCR transgene yields T cells recognizing a HEL peptide presented in the context of I-A^k (Akkaraju et al. 1997; Ho et al. 1994). To allow for effective HEL peptide presentation on I-A^k, this pair of insHEL and 3A9 TCR transgenes was introduced onto B10.BR and NOD.*H2^k* genetic backgrounds, resulting in the diabetes-resistant 3A9 TCR:insHEL B10.BR and diabetes-susceptible 3A9 TCR:insHEL NOD.*H2^k* mouse strains (Lesage et al. 2002). Importantly, 3A9 DN T cell proportion is decreased in secondary lymphoid organs of mice from the diabetes-susceptible NOD.*H2^k* background in comparison to the diabetes-resistant B10.BR background (Dugas et al. 2010), where this difference is partially restored by the presence of the *Idd2* or *Idd13* locus from the B10.BR background in NOD.*H2^k* congenic mice (Collin et al. 2014; Dugas et al. 2014).

Herein, we investigated the interactions between genetic determinants encoded within the *Idd2* and *Idd13* loci and how they influence DN T cell proportion. To do so, we generated 3A9 TCR and 3A9 TCR:insHEL NOD.*H2^k*-*Idd2/13* double congenic mice. Using the double congenic mice, we demonstrate an interaction between *Idd2* and *Idd13* loci in determining the number of DN T cells in secondary lymphoid organs, where DN T cell proportion is fully restored in the lymph nodes of 3A9 TCR:insHEL NOD.*H2^k*-*Idd2/13* mice. By exploiting DAVID and STRING bioinformatics databases, we link potential biological pathways arising from interactions of genes encoded within the *Idd2* and *Idd13* loci. This in silico

approach suggested that the *Idd2* and *Idd13* loci may regulate cell cycle progression. Using congenic mice, we validate that the *Idd2* and *Idd13* loci influence progression through S-phase and DN T cell proliferation. Moreover, we find that both the *Idd2* and *Idd13* loci modulate RAD51 expression. Together, the bioinformatics data, the cell cycle analysis, and the regulation of RAD51 expression suggests that *Idd2* and *Idd13* loci modulate cell cycle progression, which likely contributes to defining the proportion of DN T cells in secondary lymphoid organs.

Results

The proportion of 3A9 DN T cells is significantly lower in the lymph nodes of 3A9 TCR NOD.*H2^k* mice in comparison to 3A9 TCR B10.BR mice, even in the absence of cognate antigen (Dugas et al. 2010). This suggests that the NOD genetic background, independent of the autoimmune response, defines the low number of DN T cells in secondary lymphoid organs. To identify these genetic determinants, we previously performed a linkage analysis on an F2 outcross from these two parental strains and found that immunoregulatory DN T cell proportion is regulated by a multigenic trait in secondary lymphoid organs (Collin et al. 2014). By exploiting the 3A9 TCR transgenic mouse model, we subsequently demonstrated that both *Idd2* and *Idd13* loci independently contribute to defining the proportion and number of DN T cells in the spleen and lymph nodes (Collin et al. 2014; Dugas et al. 2014). Still, 3A9 TCR NOD mice congenic for either of these loci presented with a modest increase in DN T cell number relative to mice bearing the B10.BR genetic background. As a result, we proposed that interactions between genetic determinants encoded within the *Idd2* and *Idd13* loci cooperate to define the proportion and number of immunoregulatory DN T cells. We segregated the F2 mice from our aforementioned linkage analysis (Collin et al. 2014) according to their genotype at the SNP with the highest LOD score on both chromosome 2 (*Idd13*) and chromosome 9 (*Idd2*), namely rs6193859 and D9Mit232, respectively, and plotted the proportion of 3A9 DN T cells from the skin-draining lymph nodes (Fig. 1a, Table 1). F2 mice bearing NOD homozygous alleles at the *Idd2* locus present with a low proportion of DN T cells, which is not significantly influenced by the presence of either NOD or B10.BR alleles at the *Idd13* locus (Fig. 1a, white circles). However, we find a significant increase in the proportion of DN T cells in F2 mice bearing homozygous B10.BR alleles at both loci (19.34 ± 1.42) when compared to mice bearing homozygous NOD alleles at *Idd2* (13.60 ± 1.10), at *Idd13* (13.65 ± 1.36), or at both loci (11.82 ± 2.05) (Table 1). This suggests that B10.BR alleles from both *Idd2* and *Idd13* loci may have an additive or synergistic effect in regulating DN T cell proportion.

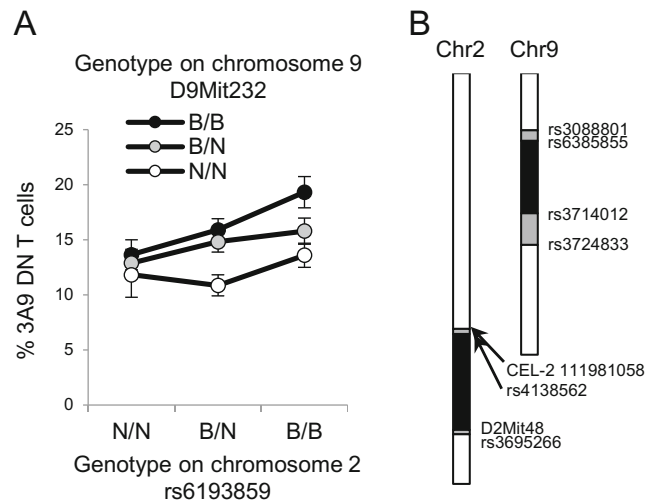


Fig. 1 Interactions between chromosome 2 and chromosome 9 in determining 3A9 DN T cell proportion in 3A9 TCR F2 mice. **a** The proportion of 3A9 DN T cells in the skin-draining lymph nodes of 3A9 TCR F2 mice is represented based on their genotype on chromosome 2 at rs6193859 (x axis) and chromosome 9 at D9Mit232 (colored circles). N/N = homozygous NOD.*H2^k* alleles, B/N = heterozygous alleles, B/B = B10.BR homozygous alleles. Black circles, homozygous B10.BR alleles at D9Mit232; gray circles, heterozygous alleles at D9Mit232; white circles, homozygous NOD.*H2^k* alleles at D9Mit232. Mean ± SEM are represented. **b** Schematic representation of mouse chromosome 2 and chromosome 9 from NOD.*H2^k*-*Idd2/13* congenic mice. The delimitation of the congenic interval as defined by Illumina medium density or PCR reaction. B10 alleles are shown in black, NOD alleles in white, and alleles of undetermined origin in gray. The markers are positioned according to assembly NCBI m37 coordinates

To test this potential interaction between *Idd2* and *Idd13* loci, we generated 3A9 TCR NOD.*H2^k*-*Idd2/13* as well as 3A9 TCR:insHEL NOD.*H2^k*-*Idd2/13* double congenic mice, where the limits of the intervals were determined by genotyping and medium density SNP Illumina platform (Fig. 1b). As previously reported, B10.BR mice present with a higher proportion of 3A9 DN T cells than NOD.*H2^k* mice in both the spleen and lymph nodes of either the 3A9 TCR single transgenic or 3A9 TCR:insHEL double transgenic mice (Fig. 2) (Collin et al. 2014; Dugas et al. 2010; Dugas et al. 2013;

Table 1 3A9 DN T cell proportion in the lymph nodes of 3A9 TCR F2 mice based on homozygous genotypes at one or both loci, specifically at rs6193859 encoded within *Idd13* and at D9Mit232 encoded within *Idd2*

<i>Idd13</i> ; <i>Idd2</i>	Mean ± SEM	vs	<i>Idd13</i> ; <i>Idd2</i>	Mean ± SEM	p value
N/N; N/N	11.82 ± 2.05	vs	B/B; N/N	13.60 ± 1.10	1.00
N/N; N/N	11.82 ± 2.05	vs	N/N; B/B	13.65 ± 1.36	1.00
N/N; N/N	11.82 ± 2.05	vs	B/B; B/B	19.34 ± 1.42	0.011
B/B; N/N	13.60 ± 1.10	vs	N/N; B/B	13.65 ± 1.36	1.00
B/B; N/N	13.60 ± 1.10	vs	B/B; B/B	19.34 ± 1.42	0.039
N/N; B/B	13.65 ± 1.36	vs	B/B; B/B	19.34 ± 1.42	0.033

*p value <0.05; ns: non-significant based on Bonferroni’s Multiple Comparison Test

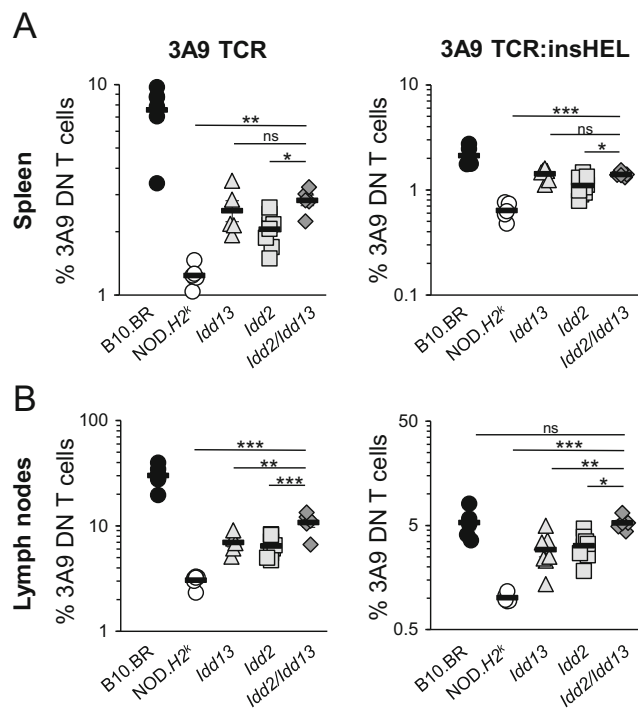


Fig. 2 The *Idd2* and *Idd13* loci cooperate to define the proportion of 3A9 DN T cells in lymph nodes. The proportion of 3A9 DN T cells is shown for 3A9 TCR and 3A9 TCR:insHEL transgenic mice in the spleen (**a**) and the lymph nodes (**b**). Each dot represents data from one mouse. Mean \pm SEM are shown. p value * < 0.05 , ** < 0.01 , *** < 0.001 according to one-way ANOVA with Bonferroni post-hoc test. ns, non-significant

Dugas et al. 2014; Hillhouse et al. 2010). In addition, both the *NOD.H2^k-Idd2* and *NOD.H2^k-Idd13* single congenic mice show an increase in the proportion of 3A9 DN T cells relative to *NOD.H2^k* mice (Fig. 2) (Collin et al. 2014; Dugas et al. 2014). Although the proportion of 3A9 DN T cells was increased in the spleen of *NOD.H2^k-Idd2/13* double congenic mice relative to the parental *NOD.H2^k* strain, the proportion of 3A9 DN T cells of the double congenic mice did not exceed that of *NOD.H2^k-Idd13* single congenic mice in the spleen (Fig. 2a). In contrast to the spleen, and in agreement with the F2 linkage data of 3A9 DN T cells in the lymph nodes (Fig. 1), we observe a statistically significant increase in the proportion of 3A9 DN T cells of *NOD.H2^k-Idd2/13* double congenic mice compared to single congenic mice in the lymph nodes (Fig. 2b). Importantly, the proportion of 3A9 DN T cells in the lymph nodes of 3A9 TCR:insHEL *NOD.H2^k-Idd2/13* double congenic mice was comparable to that of the 3A9 TCR:insHEL B10.BR parental strain (Fig. 2b). Notably, the increased proportion of 3A9 DN T cells in the lymph nodes of *NOD.H2^k-Idd2/13* double congenic mice relative to *NOD.H2^k*, although not as striking, is corroborated in absolute numbers (Fig. 3), and is not the result of a decrease in the proportion of either CD4 or CD8 T cells (Table 2). Together, these data suggest that an interaction between *Idd2* and *Idd13*

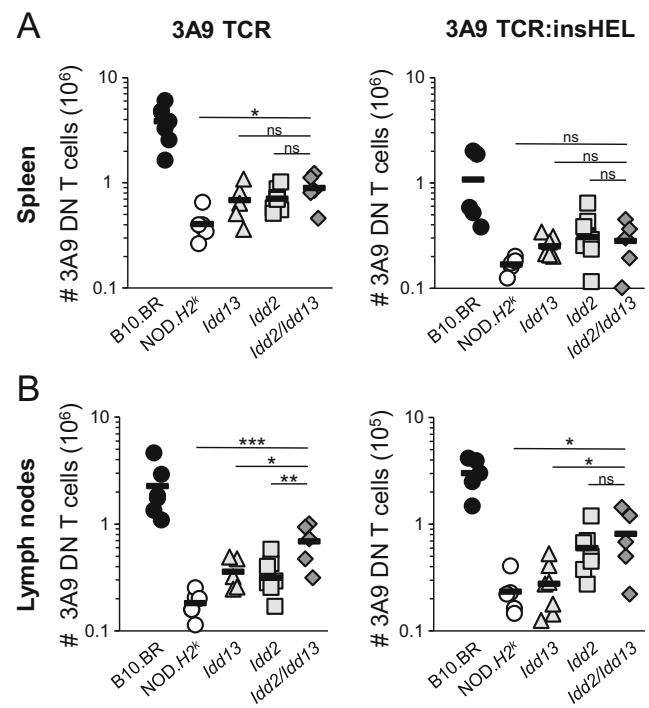


Fig. 3 The *Idd2* and *Idd13* loci cooperate to define the absolute number of 3A9 DN T cells in lymph nodes. The absolute number of 3A9 DN T cells is shown for 3A9 TCR and 3A9 TCR:insHEL transgenic mice in the spleen (**a**) and the lymph nodes (**b**). Each dot represents data from one mouse. Mean \pm SEM are shown. p value * < 0.05 , ** < 0.01 , *** < 0.001 according to one-way ANOVA with Bonferroni post-hoc test. ns, non-significant

loci increases the proportion of 3A9 DN T cells in the *NOD.H2^k* transgenic mice.

The increased proportion of 3A9 DN T cells in secondary lymphoid organs of *NOD.H2^k-Idd2/13* double congenic mice relative to that of *NOD.H2^k* mice may potentially result from an increase in thymic selection in the 3A9 TCR:insHEL *NOD.H2^k-Idd2/13* mice. We thus quantified the proportion of 3A9 DN T cells in the thymus of the various 3A9 TCR single transgenic and 3A9 TCR:insHEL double transgenic mice. As for the spleen and lymph nodes, we find a higher proportion and absolute number of 3A9 DN T cells in the thymus of B10.BR mice relative to *NOD.H2^k* mice, in both the 3A9 TCR single transgenic and 3A9 TCR:insHEL double transgenic mice (Fig. 4). In addition, the *NOD.H2^k-Idd13* single congenic mice show a modest increase in the proportion of 3A9 DN T cells relative to *NOD.H2^k* mice, whereas the increase in 3A9 DN T cells for *NOD.H2^k-Idd2* is only observed in the 3A9 TCR:insHEL double transgenic mice (Fig. 4). Notably, although the proportion and absolute number of 3A9 DN T cells was modestly increased in the thymus of *NOD.H2^k-Idd2/13* double congenic mice relative to *NOD.H2^k* mice, this increase was comparable to that observed in the *NOD.H2^k-Idd13* single congenic mice (Fig. 4). This suggests the absence of an additive effect of the *Idd2* and *Idd13* loci in defining DN T cell number in the thymus. In line

Table 2 Proportion of 3A9 CD4⁺ and 3A9 CD8⁺ T cells in the spleen and lymph nodes of 3A9 TCR and 3A9 TCR:insHEL mice in each strain, as indicated. Mean ± SD from at least four mice per group is shown

		3A9 TCR		3A9 TCR:insHEL	
		% 3A9 CD4 T cells	% 3A9 CD8 T cells	% 3A9 CD4 T cells	% 3A9 CD8 T cells
Spleen	B10.BR	4.43 ± 3.20	1.22 ± 0.52	0.21 ± 0.08	0.12 ± 0.07
	NOD.H2 ^k	5.91 ± 3.27	0.79 ± 0.18	1.47 ± 0.98	0.16 ± 0.04
	NOD. <i>Idd13</i>	6.62 ± 2.26	1.6 ± 0.47	1.82 ± 1.26	0.48 ± 0.08
	NOD. <i>Idd2</i>	6.58 ± 4.59	1.54 ± 0.52	1.61 ± 2.9	0.5 ± 0.28
	NOD. <i>Idd2-Idd13</i>	4.15 ± 2.10	1.07 ± 0.32	0.64 ± 0.35	0.36 ± 0.12
Lymph nodes	B10.BR	9.52 ± 5.68	4.04 ± 1.72	0.24 ± 0.12	0.53 ± 0.33
	NOD.H2 ^k	15.15 ± 6.18	2.78 ± 0.69	2.72 ± 2.56	0.86 ± 0.38
	NOD. <i>Idd13</i>	17.24 ± 6.44	5.85 ± 1.65	2.69 ± 2.07	1.83 ± 0.68
	NOD. <i>Idd2</i>	15.11 ± 7.91	5.52 ± 1.71	1.07 ± 1.3	1.44 ± 0.67
	NOD. <i>Idd2-Idd13</i>	8.87 ± 3.80	4.41 ± 0.79	0.81 ± 0.52	1.47 ± 0.40

with our previous work showing that thymic DN T cell proportion in 3A9 TCR mice does not correlate with 3A9 DN T cell proportion in secondary lymphoid organs (Dugas et al. 2013), we find that the increased proportion of 3A9 DN T cells in the secondary lymphoid organs of NOD.H2^k-*Idd2/13*

double congenic mice relative to NOD.H2^k mice is not a consequence of increased thymic differentiation towards the DN T cell lineage.

In the 3A9 TCR:insHEL B10.BR, BALB.K, and NOD.H2^k mice, we have previously shown that elevated numbers 3A9 DN T cells in secondary lymphoid organs correlate with a decrease in diabetes incidence and that injection of 3A9 DN T cells in the BALB.K setting is sufficient to prevent diabetes onset (Dugas et al. 2010). We have also shown that 3A9 TCR:insHEL NOD.H2^k-*Idd2* mice exhibit an increase in 3A9 DN T cells and a lower incidence of diabetes relative to 3A9 TCR:insHEL NOD.H2^k mice (Collin et al. 2014). However, we recently found that 3A9 TCR:insHEL NOD.H2^k-*Idd13* mice, which present an increase in 3A9 DN T cells relative to their NOD.H2^k counterpart (Fig. 2) (Dugas et al. 2014), exhibit an increase in diabetes incidence (Hillhouse et al. 2016). This result suggests that, in contrast to *Idd2*, the increase in DN T cell number conferred by the *Idd13* locus is not sufficient to control insulinitis present in the 3A9 TCR:insHEL mouse model (as detailed in (Hillhouse et al. 2016)). Because of the contrasting phenotypes of *Idd2* and *Idd13* in controlling diabetes incidence in 3A9 TCR:insHEL NOD.H2^k mice, we decided to study the impact of the combination of both *Idd2* and *Idd13* loci. Expectedly, 3A9 TCR:insHEL NOD.H2^k-*Idd2/13* double congenic mice presented a level of insulinitis that was comparable to both 3A9 TCR:insHEL B10.BR and NOD.H2^k mice (Fig. 5). Still, all of the nine 3A9 TCR:insHEL NOD.H2^k-*Idd2/13* mice that were aged to over 28 weeks remained diabetes-free and never exhibited glucosuria nor glycemia (Table 3). The combination of the *Idd2* and *Idd13* loci in the 3A9 TCR:insHEL NOD.H2^k mice also significantly reduced the serum level of HEL-specific IgG autoantibodies (Table 3). Taken together, these data show that the combined presence of *Idd2* and *Idd13* loci in 3A9 TCR:insHEL NOD.H2^k mice enhances the proportion

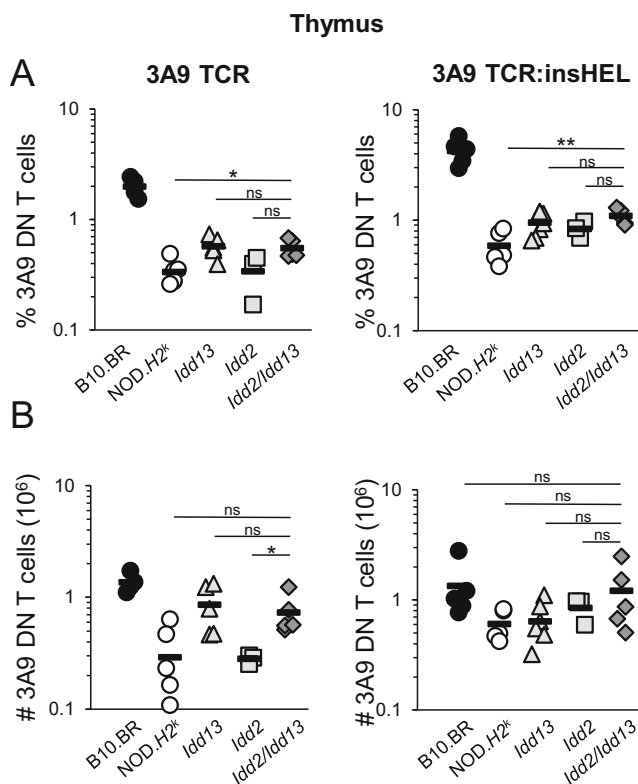


Fig. 4 The impact of *Idd2* and *Idd13* loci on the proportion and number of 3A9 DN T cells in secondary lymphoid organs is not due to increased thymic differentiation. The proportion (a) and absolute number (b) of 3A9 DN T cells in the thymus is shown for 3A9 TCR and 3A9 TCR:insHEL transgenic mice. Each dot represents data from one mouse. Mean ± SEM are shown. *p* value * < 0.05, ** < 0.01 according to one-way ANOVA with Bonferroni post-hoc test. ns, non-significant

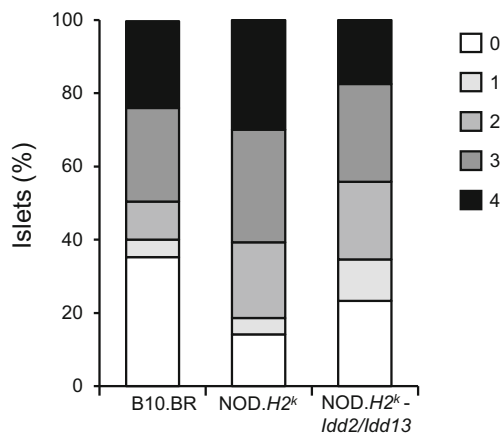


Fig. 5 Insulinitis is not affected by the combination of *Idd2* and *Idd13* loci in 3A9 TCR:insHEL mice. The degree of islet infiltration is shown for euglycemic male and female mice of 8–14 weeks old. B10.BR ($n = 5$), NOD.H2^k ($n = 4$), and NOD.H2^k-*Idd2*/*Idd13* mice ($n = 5$)

of 3A9 DN T cells in secondary lymphoid organs and decreases the level of autoantibodies, as well as prevents diabetes onset.

We next sought to define the biological process related to the increase in DN T cell proportion which is mediated by the combination of the *Idd2* and *Idd13* congenic intervals. We considered all of the genes encoded within the *Idd2* and *Idd13* loci. We then queried the DAVID bioinformatics database based on the gene list from the *Idd2* and *Idd13* loci. The *Idd2* and *Idd13* gene lists independently revealed nine and five biological processes respectively, while 11 biological processes were identified by the combination of the two gene lists (Table 4). Using the combined *Idd2* and *Idd13* gene lists obtained by the DAVID analysis, we next independently queried the STRING database for each of these 11 biological processes. We selectively considered associations from genes in *Idd2* and *Idd13* that showed a confidence score above 0.7 for the given biological process (Table 5). We find strong interactions between genes in all biological processes, except for lipid transport where the four links between genes from *Idd2* and *Idd13* all presented with a confidence below 0.7. Based on this observation, we decided to further restrict our attention to biological processes where a confidence score above 0.7 was given to most of the gene interactions (i.e., more than 50% of the interactions). Out of the 11 biological processes,

only 3 fit these criteria, namely phospholipid catabolism, T cell, and cell cycle (Table 5, highlighted in gray).

The DAVID analysis grouped 7 genes from the *Idd2* locus and 28 genes from the *Idd13* locus under phospholipid catabolism. STRING revealed that only two genes from the *Idd2* locus, namely *Arhgef12* and *Pafah1b2*, were associated with genes from the *Idd13* locus (Fig. 6a). Accordingly, *Arhgef12* was linked to *Adra1d* while *Pafah1b2* was linked to four genes of the *Pla2g4* family, specifically *Pla2g4b*, *Pla2g4d*, *Pla2g4e*, and *Pla2g4f*. Based on ImmGen, *Arhgef12* is strongly expressed in germinal center B cells and *Pafah1b2* is expressed in many immune cell populations (immgen.org). However, neither *Adra1d* nor any of the four *Pla2g4* genes from the *Idd13* locus are expressed in hematopoietic cells (immgen.org). As we have previously shown that DN T cell proportion is regulated at least in part by hematopoietic-intrinsic factors (Dugas et al. 2014), it is unclear how the *Arhgef12* and *Pafah1b2* genes from the *Idd2* locus interact with *Adra1d* or any of the four *Pla2g4* genes from the *Idd13* locus to influence the proportion of DN T cells, as none of the potentially interacting genes in *Idd13* are expressed in the hematopoietic system.

The T cell biological process showed interactions between genes from the CD3 complex encoded in the *Idd2* locus and *B2m* from the *Idd13* locus (Fig. 6b). This interaction stems from the antigen presentation of peptides to CD8⁺ T cells, where the chains of the CD3 complex are necessary for TCR expression which recognizes peptides in the context of MHC class I molecules that are associated with $\beta 2m$. However, we have previously demonstrated that *B2m* deficiency does not decrease the proportion of 3A9 DN T cells in both the spleen and lymph nodes of 3A9 TCR transgenic mice, as shown in *B2m*-deficient mice from both B10.BR and NOD.H2^k genetic backgrounds (Dugas et al. 2014). The T cell biological process is thus unlikely to explain the additive interaction between *Idd2* and *Idd13* loci in defining the proportion of DN T cells.

Finally, STRING analysis of the cell cycle progression reveals multiple relevant interactions between genes from the *Idd2* and *Idd13* loci (Fig. 6c). For one, *Chek1* in *Idd2* partners with *Rad51*, *Mcm8*, and *Cdc25b* in *Idd13* to regulate cell cycle progression (Kramer et al. 2004; Lutzmann et al. 2012; Patil et al. 2013; Sorensen et al. 2005). In addition, *Zw10* in *Idd2*

Table 3 Serum antibodies (relative units) and diabetes incidence of 3A9 TCR:insHEL mice from the different strains

	B10.BR	NOD.H2 ^k	NOD.H2 ^k - <i>Idd2</i> / <i>Idd13</i>
Levels of total IgG	15.85 ± 4.06	10.34 ± 2.20	7.80 ± 2.35
Levels of IgG anti-HEL	0.45 ± 0.45	3.12 ± 0.90	1.49 ± 0.41
Levels of IgG1 anti-HEL	0.15 ± 0.12	0.57 ± 0.18	0.23 ± 0.07
Diabetes incidence (%)	25 ^{a, b}	60–80 ^{a, b, c}	0

^a Lesage, Goodnow, JEM (2002)

^b Collin et al., JI (2014)

^c Hillhouse et al., ICB (2016)

Table 4 Biological pathways present in *Idd2*, *Idd13* or in both loci

<i>Idd2</i>	<i>Idd13</i>	<i>Idd2</i> and <i>Idd13</i>
Cell junction and synapse	Cell cycle	Microtubules and cytoskeleton
Dendrite	Intracellular organelle	Cell cycle
DNA checkpoint	Response to stress	Nucleotide process
Glycosylation	Signal process	Phospholipid catabolic process
Immune system development	Cilium formation	Protease inhibitor
Ions transport and voltage		Carbohydrate metabolism
Lipid metabolic process		Ig-like domain
Negative regulation of motion		Lipid transport
Protease		Signal protein
		T cell
		Endoplasmic reticulum membrane

and *Bub1*, *Bub1b*, and *Casc5* in *Idd13* all localize to the kinetochore and facilitate mitotic progression (Anderson et al. 2002; Genin et al. 2012; Taylor and McKeon 1997; Vallee et al. 2006; Varma et al. 2006). Importantly, all of these genes are ubiquitously expressed.

To determine if cell cycle progression is possibly impaired in NOD.*H2^k* and could therefore define DN T cell number, we performed cell cycle analysis using propidium iodide staining in total spleen cells from B10.BR, NOD.*H2^k* and NOD.*H2^k-Idd2/13* mice. A greater proportion of cells from NOD.*H2^k* mice were actively engaged in S-phase (Fig. 7a). Interestingly, cells from NOD.*H2^k-Idd2/13* mice exhibited a comparable cell cycle profile to that of B10.BR mice with a similar proportion of cells in S-phase (Fig. 7a). This finding suggests that the *Idd2* and *Idd13* loci on the NOD.*H2^k* background are sufficient to modulate the proportion of cells in S-phase. We confirm that this is not a particularity of the MHC haplotype, as we find that spleen cells from NOD mice also have a higher proportion of cells in S-phase relative to those from C57BL/6 mice (Fig. 7b). More importantly, we find that, among T cell subsets, the impact of the *Idd2* and *Idd13* loci on proliferation is specific to DN T cells (Fig. 7c). Indeed, when comparing T

cell subsets from both NOD.*H2^k* and NOD.*H2^k-Idd2/13* mice, we find a similar proportion of either CD4⁺ or CD8⁺ T cells that express Ki-67. However, a lower proportion of DN T cells from NOD.*H2^k-Idd2/13* mice stained positive for Ki-67 relative to DN T cells from NOD.*H2^k* mice (Fig. 7c). As for S-phase measurements, the fraction of Ki-67⁺ DN T cells from NOD.*H2^k-Idd2/13* mice is comparable to that of B10.BR mice. Altogether, these data suggest that the low proportion of DN T cells in the NOD background is influenced by allelic variants of genes encoded within the *Idd2* and *Idd13* loci, which together influence the cell cycle of immunoregulatory DN T cells.

Progression of DN T cells through the cell cycle is influenced by the *Idd2* and *Idd13* loci. Of the candidate genes encoded within *Idd13*, our attention turned to *Rad51*, as inhibition of RAD51 has recently been shown to inhibit diabetes development (Ratiu et al. 2017). RAD51 is a recombinase involved in DNA repair, an essential step to allow efficient progression through the cell cycle. RAD51 acts downstream of γ -H2AX and CHEK1, both of which are encoded within *Idd2*. Interestingly, we found that RAD51, but not γ -H2AX, was expressed more abundantly in spleen cells from

Table 5 Summary of interactions between genes in *Idd2* and *Idd13* loci

	Number of gene interactions with >0.7 confidence score	Percentage of interactions with >0.7 confidence score
Phospholipid catabolism	5	71.4%
T cell	2	66.7%
Cell cycle	15	51.7%
Carbohydrate metabolism	5	45.5%
Microtubules and cytoskeleton	10	41.7%
Ig-like domain	3	33.3%
Signal protein	20	26.7%
Protease inhibitor	2	22.2%
Nucleotide process	12	11.8%
Endoplasmic reticulum membrane	1	10.0%
Lipid transport	0	0.0%

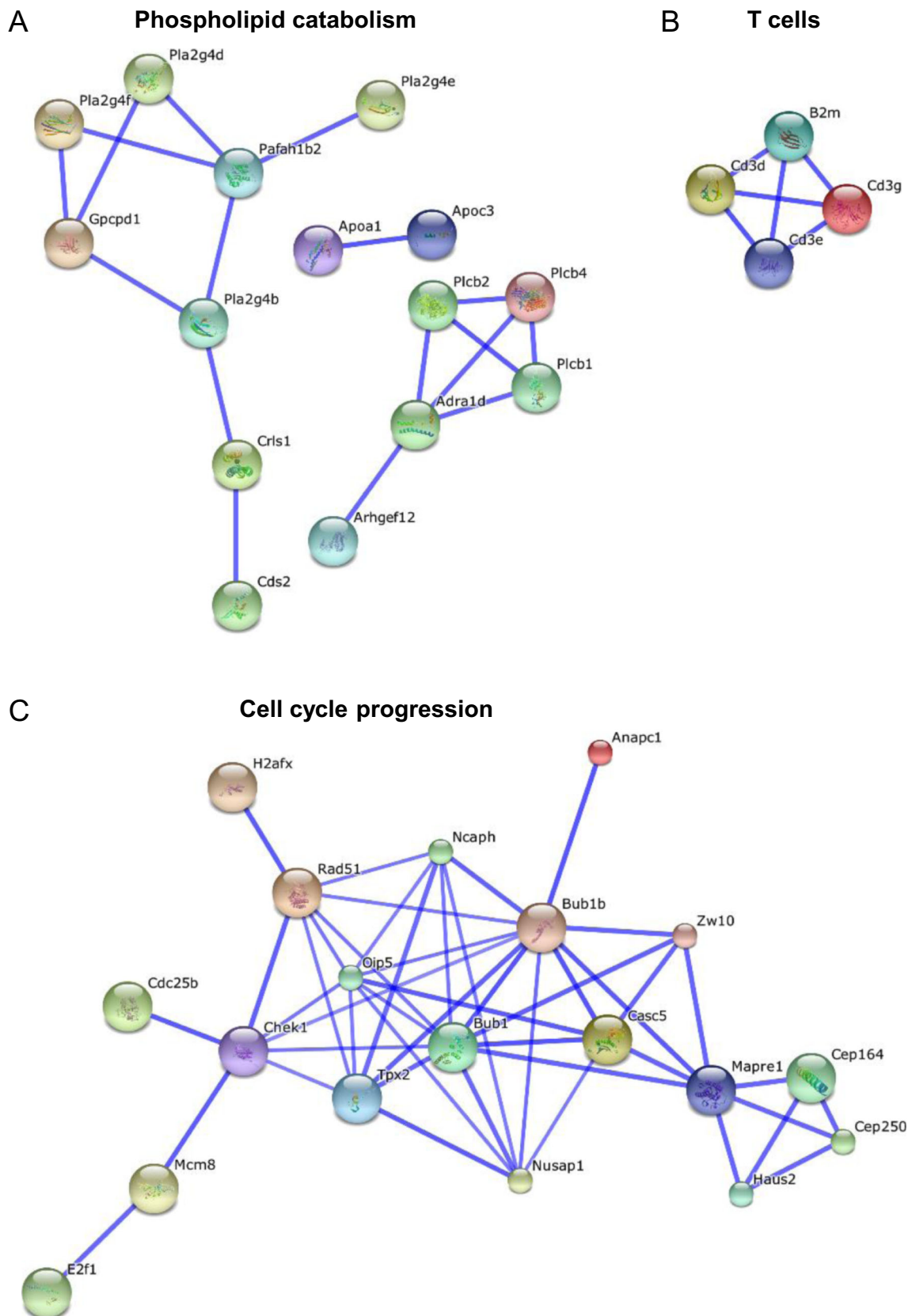


Fig. 6 STRING analysis of gene lists grouped under biological pathways revealed by DAVID. **a** Phospholipid catabolic process; **b** T cells; and **c** cell cycle progression, showing the confidence level of protein interaction for genes encoded within the *Idd2* and *Idd13* loci

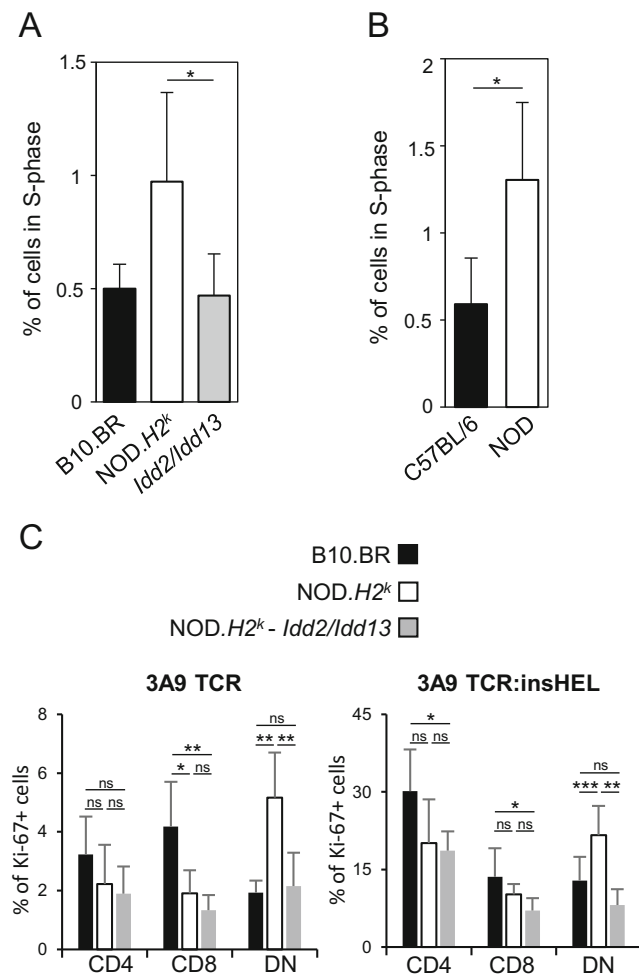


Fig. 7 Allelic variants in the *Idd2* and *Idd13* loci influence cell cycle. Total spleen cells were stained with propidium iodide and the percentage of cells in S-phase was quantified by flow cytometry, for **a** B10.BR, NOD.H2^k and NOD.H2^k-*Idd2*/*Idd13* mice (*n* = 5) and **b** C57BL/6 (B6) and NOD mice (*n* = 7). Mean ± SEM are shown. **c** Spleen cells from B10.BR and NOD.H2^k-*Idd2*/*Idd13* mice were stained with antibodies to CD3, CD4, CD8, and Ki-67. The percentage of Ki-67⁺ cells was quantified for CD4⁺ (CD3⁺CD4⁺CD8⁻), CD8⁺ (CD3⁺CD4⁻CD8⁺), and DN (CD3⁺CD4⁻CD8⁻) T cells. *n* = 5. Mean ± SEM are shown. Student *t* test, *p* value * < 0.05, ** < 0.01, *** < 0.001, ns = non-significant

NOD.H2^k mice relative to B10.BR mice (Fig. 8 and data not shown). We also found that NOD.H2^k mice carrying either the *Idd2* or the *Idd13* locus both showed a reduction in RAD51 expression, which was not enhanced in NOD.H2^k-*Idd2*/*Idd13* mice (Fig. 8). This result suggests that polymorphisms within the *Idd13* locus, which encodes for *Rad51*, effectively modulate RAD51 expression. Importantly, it also suggests that polymorphisms in the *Idd2* locus, likely in either *H2afx* or *Chek1*, also impact RAD51 expression. Yet, the polymorphism in both *Idd2* and *Idd13* did not cooperate to restore RAD51 expression to the levels observed in B10.BR mice, suggesting that although *Idd2* and *Idd13* clearly regulate RAD51 expression, other pathways are also affected by the two loci.

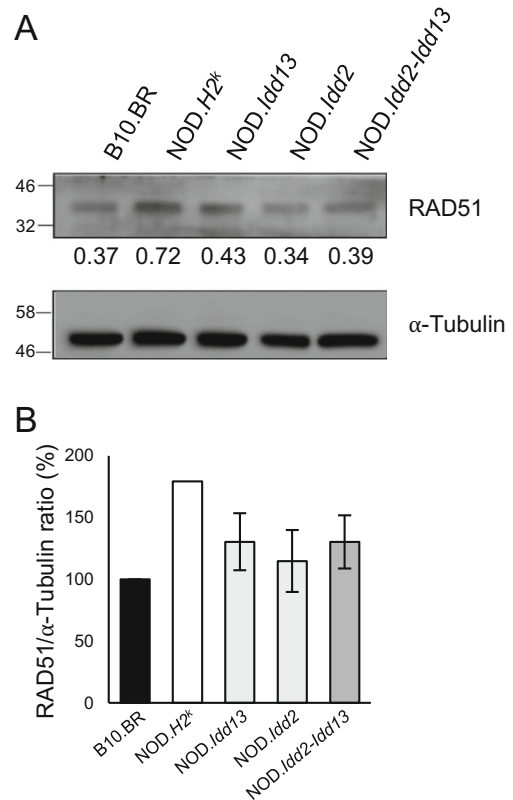


Fig. 8 RAD51 expression is modulated by polymorphisms on both the *Idd2* and *Idd13* loci. One representative Western blot (**a**) and data compilation (**b**) of relative RAD51 protein levels in total spleen cells from B10.BR, NOD.H2^k, NOD.H2^k-*Idd2*, NOD.H2^k-*Idd13*, and NOD.H2^k-*Idd2*/*Idd13* (*n* = 3). alpha-tubulin is used as a loading control.

Discussion

We have previously shown that autoimmune diabetes susceptibility is associated with decreased DN T cell proportion (Collin et al. 2014; Dugas et al. 2010). In order to identify the genetic determinants defining DN T cell number, we used a linkage analysis approach and congenic strain validation and demonstrated that DN T cell proportion is influenced by *Idd2* and *Idd13* (Collin et al. 2014; Dugas et al. 2014). However, as the contribution of each locus was modest, we sought to investigate the interactions between the genetic determinants encoded within *Idd2* and *Idd13* loci and how they cooperate to define DN T cell numbers. Here, we analyzed our linkage analysis data (Collin et al. 2014) and revealed that F2 mice bearing homozygous B10.BR alleles at both the *Idd2* and *Idd13* loci exhibit a significant increase in DN T cell proportion when compared to mice bearing homozygous NOD alleles at either or both loci. In addition, we show that *Idd2* and *Idd13* together increase the proportion of DN T cells in both 3A9 TCR and 3A9 TCR:insHEL NOD.H2^k mice. Moreover, in a cohort of nine female mice, none of the 3A9 TCR:insHEL NOD.H2^k-*Idd2*/*Idd13* mice develop autoimmune diabetes. Together, these data suggest an additive effect of the mouse

Idd2 and *Idd13* loci in the restoration of DN T cells, a trait associated with autoimmune diabetes resistance. Lastly, we demonstrated that cell cycle and DN T cell proliferation are regulated by the *Idd2* and *Idd13* loci. Together with our bioinformatics analysis, this suggests that cell cycle progression, by modulating RAD51 expression, is likely contributing to defining the proportion of DN T cells in secondary lymphoid organs.

Of interest, RAD51 has recently been linked to type 1 diabetes (Ratiu et al. 2017). In this study, they find that inhibiting RAD51 protects from diabetes development by enhancing the proportion of immunoregulatory B cells. Notably, DN T cells are able to eliminate B cells and in vivo injection of DN T cells leads to a decrease in autoantibody levels (Dugas et al. 2010; Hillhouse et al. 2010; Ma et al. 2008). It is thus tempting to suggest that inhibiting RAD51 leads to a specific increase in DN T cells which would eliminate autoantibody-producing B cells, thereby resulting in a proportional increase in immunoregulatory B cells, altogether preventing autoimmune diabetes onset. Alternatively, as we have shown that RAD51 is generally increased in the spleen of NOD mice, inhibiting RAD51 may independently affect many cell types, all actively participating in the induction or maintenance of immune tolerance.

Identifying the molecular pathways that influence the size of the DN T cell pool in peripheral lymphoid organs is of interest as it will facilitate the identification of molecular targets that regulate DN T cell numbers. During our analysis of DAVID and STRING bioinformatics databases exploiting the *Idd2* and *Idd13* gene lists, we were able to limit our focus on three biological processes mediated by strong interactions of genes within the two loci, namely phospholipid catabolism, T cell biology, and cell cycle progression. However, concerning phospholipid catabolism, the five genes located within the *Idd13* locus that were found to interact with genes from the *Idd2* locus, specifically *Adra1d*, *Pla2g4b*, *Pla2g4d*, *Pla2g4e*, and *Pla2g4f*, are not expressed in hematopoietic cells (immgen.org). As we have previously shown that DN T cell proportion is regulated at least in part by hematopoietic-intrinsic factors (Dugas et al. 2014), we found it unlikely that the phospholipid catabolism is the biological process influencing DN T cell numbers. Likewise, the T cell biological process was highlighted by interactions between genes from the CD3 complex encoded in the *Idd2* locus and *B2m* from the *Idd13* locus, where we have previously shown that *B2m*-deficiency does not influence 3A9 DN T cell proportion in secondary lymphoid organs (Dugas et al. 2014). Therefore, the T cell biological process is not likely influencing DN T cell numbers. As a result, we shifted our focus to the third biological process highlighted by our bioinformatics analyses, cell cycle. The STRING analysis of the cell cycle progression revealed several relevant interactions between genes from the *Idd2* and *Idd13* loci, with various genes of interest being ubiquitously

expressed. We further validate that cell cycle and proliferation are regulated by the *Idd2* and *Idd13* loci as a greater proportion of lymphocytes from NOD.*H2^k* mice are in S-phase. Moreover, the proportion of Ki-67⁺ DN T cells is also increased in NOD.*H2^k* mice in comparison to both B10.BR and NOD.*H2^k*-*Idd2/13* mice. The greater proportion of proliferating DN T cells in NOD.*H2^k* mice, which exhibit a lower proportion of DN T cells in lymphoid organs, relative to NOD.*H2^k*-*Idd2/13* mice is counterintuitive. However, the increased proportion of cells in S-phase may suggest a block in cell cycle progression, yielding lower numbers of DN T cells. Altogether, our data thus suggest that DN T cell proportion is influenced by allelic variants of genes encoded within the *Idd2* and *Idd13* loci, which together influence cell cycle progression.

The cell cycle consists of a series of sequential phases, specifically the G₀/G₁, S, G₂, and M (mitosis) phases, leading to cell division. During the cell cycle, multiple checkpoints are encountered prior to entry into the subsequent phase, which provides an important surveillance mechanism for faithful replication and division of cells (Elledge 1996). The STRING analysis of the cell cycle progression revealed that *Chek1* in *Idd2* partners with *Rad51*, *Mcm8*, and *Cdc25b* from the *Idd13* locus. Indeed, each of these four genes play an important role during S-phase by controlling DNA replication and the DNA damage response to replicative stress. For instance, the DNA helicase MCM8 is a significant player in the elongation phase of DNA replication (Maiorano et al. 2005), it promotes RAD51 recruitment to DNA damage sites and it facilitates homologous recombination-mediated repair of DNA double-strand breaks (Park et al. 2013). As RAD51 is central in replication fork progression (Berti and Vindigni 2016), MCM8 may participate in this pathway during S-phase. In addition to MCM8, *Cdc25b*, which encodes a phosphatase that is essential for cell cycle transition by promoting the dephosphorylation of key substrates (Lammer et al. 1998), is also a key player during S-phase. For instance, down-regulation of *Cdc25* mRNA levels in HeLa cells delays S-phase and leads to a proliferation defect (Garner-Hamrick and Fisher 1998). Furthermore, CDC25B has been involved in centrosome duplication, a process that is initiated in S-phase (Boutros et al. 2007). Interestingly, unscheduled expression of CDC25B during DNA replication has been linked to replicative stress and the formation of DNA lesions (Bugler et al. 2010). In this regard, CHEK1 also plays a dual role during DNA replication. Indeed, CHEK1 is linked to fork progression during S-phase by controlling the initiation of DNA replication (Petermann et al. 2010), and is also critical in the response to single-stranded DNA lesions by phosphorylating key substrates, including the CDC25 phosphatases, and promoting the activation of DNA damage checkpoints (Patil et al. 2013). Interestingly, the conditional deletion, knockdown, or inhibition of *Chek1* is associated with an

accumulation of cells in S-phase cells as well as increased cell death (Lam et al. 2004; Sorensen et al. 2005), which mirrors our observations for DN T cells from mice exhibiting NOD alleles for *Idd2* and *Idd13*. Indeed, our findings suggest that the *Idd2* and *Idd13* loci regulate the proportion of cells accumulating in S-phase and of Ki-67⁺ DN T cells. Moreover, we find that NOD.*H2^k* mice carry fewer DN T cells than both B10.BR and NOD.*H2^k*-*Idd2/13* mice in the transgenic setting and that this difference in number may be regulated, at least in part, by apoptosis (Hillhouse et al. 2010). Interestingly, CHEK1 phosphorylates RAD51 at serine-309 and recruits it to DNA repair foci in order to promote homologous recombination repair and cell survival (Sorensen et al. 2005). The fact that we observe increased RAD51 levels in the NOD.*H2^k* mice and that RAD51 is central during S-phase argues for a model where dysregulation of RAD51 levels impairs progression of DN T cells through S-phase resulting in a block in their cell cycle progression. Consequently, these results suggests that potential genetic polymorphisms influencing the interactions between genes encoded within *Idd2*, such as *Chek1*, and those encoded within *Idd13*, such as *Rad51*, *Mcm8*, and *Cdc25b*, modulate DN T cell number.

In summary, our data clearly demonstrates an interaction between the *Idd2* and *Idd13* loci in determining the number of DN T cells in secondary lymphoid organs, where DN T cell proportion and number are increased in the 3A9 TCR:insHEL NOD.*H2^k*-*Idd2/13* mice relative to both single congenic mice and to 3A9 TCR:insHEL NOD.*H2^k*. Our findings also suggest that the S-phase is likely contributing to defining the proportion of DN T cells in secondary lymphoid organs. Although cell cycle progression was the biological process that we identified through our bioinformatics approach, we cannot exclude that other pathways contribute to defining the proportion of DN T cells in secondary lymphoid organs. Further investigation of NOD.*H2^k*-*Idd2/13* double congenic mice may reveal other relevant pathways as a target for potentiating the number of immunoregulatory DN T cells, which may be of clinical use for the antigen-specific treatment of various autoimmune pathologies.

Materials and methods

Mice

3A9 TCR transgenic and HEL transgenic mice, where HEL is expressed under the rat insulin promoter (insHEL), on B10.BR and NOD.*H2^k* backgrounds have been previously described (Lesage et al. 2002). The 3A9 TCR NOD.*H2^k*-*Idd2* congenic strain bears B10.BR alleles on chromosome 9 between 29.4 and 50.0 Mb (corresponding to markers rs6385855 and rs13480186) at a locus included within *Idd2* and was

described elsewhere (Collin et al. 2014). *Idd13* congenic mice were a gift of D.V. Serreze and were crossed to NOD.*H2^k* 3A9 TCR:insHEL background to introduce the transgenes (Dugas et al. 2014). The NOD.*H2^k*-*Idd2/Idd13* strain was obtained by an intercross between 3A9 TCR:insHEL NOD.*H2^k*-*Idd2* mice and 3A9 TCR:insHEL NOD.*H2^k*-*Idd13* mice. Offspring were genotyped using the markers D9Mit129, D9Mit328, D2Mit132, D2Mit48, and D2Mit338. Mice bearing B10.BR alleles at all of these markers were selected for further intercrosses. After two generations of homozygous mating, an Illumina medium density linkage, serviced through The Centre for Applied Genomics at the Hospital for Sick Children, was performed on the tail DNA from congenic mice to delimit the boundaries of both the *Idd2* and *Idd13* loci in the NOD.*H2^k*-*Idd2/dd13* mice; *Idd2* (chromosome 9:29.6–61.4 Mb) and *Idd13* (chromosome 2:114.0–156.1 Mb) where positions are based on NCBI Build m38. All of the mouse strains were maintained at the Maisonneuve-Rosemont Hospital animal house facility (Montreal, Canada).

Flow cytometry

Eight- to 12-week-old non-diabetic mice (diastix negative) were analyzed. Spleen, lymph nodes, and thymus were pressed through a 70- μ m cell strainer (Thermo Fisher Scientific, Ottawa, Ontario, Canada). Spleen cell suspensions were treated with NH₄Cl to lyse red blood cells. Single cell suspensions were stained with the following antibodies to quantify 3A9 DN T cells: CD3 (17A2; Biolegend), TCR β (H57-597, Biolegend), CD4 (GK1.5; Biolegend and eBioscience), CD8 α (53-6.7; Biolegend), CD19 (6D5; Biolegend), and anti-clonotypic 1G12 (homemade) (Peterson et al. 1999) antibody followed by detection with IgG1 (RMG1-1; Biolegend). For Ki-67, cells were subsequently permeabilized using the eBioscience FoxP3 staining kit according to the manufacturer's protocol. Following permeabilization, cells were incubated with either Ki-67 (B56, BD) or its isotype control (IgG1 κ ; BD) for 30 min at 4 °C. For propidium iodide, single cell suspensions from the spleen were washed in PBS and thoroughly resuspended in cold 70% ethanol for at least 1 h at 4 °C. Cells were resuspended in 250 μ l of propidium iodide solution (40 μ g/ml propidium iodide, Invitrogen; 4 μ g/ml RNase, USBiological life sciences; diluted in PBS) per 1 million cells. Stained cells were kept on ice and rapidly processed on a flow cytometer. All data were collected either on a FACSCanto, LSRII, Fortessa x-20, or a BD FACSCalibur (BD Biosciences, Mississauga, Ontario, Canada). All data was analyzed with FlowJo software (Treestar, Ashland, OR, USA).

Histology

H&E staining was performed on 5 to 7 μm pancreas cuts from paraffin blocks, for two to three non-successive cuts for each mouse. H&E slides were scored for infiltration as previously described (Hillhouse et al. 2013), and according to the following scale: 0 = no infiltration, 1 = peri-insulinitis, 2 = infiltration < 50%, 3 = infiltration > 50%, 4 = complete infiltration.

ELISA

Total IgG was measured by ELISA according to the manufacturer's protocol (Bethyl Laboratories Inc., Montgomery, TX, USA). Serum anti-HEL IgG and IgG1 levels were measured by ELISA on Nunc Maxisorp plates (Thermo Fisher Scientific) coated with 100 $\mu\text{g}/\text{ml}$ HEL prepared in NaHCO_3 at pH 9.5, developed with goat anti-mouse IgG-HRP (Biolegend, clone poly4053) or rat anti-mouse IgG1-biotin (Biolegend, clone RMG1-1) followed by avidin-HRP (Biolegend). A reference pool of sera from diabetic and non-diabetic TCR:iHEL mice was set to contain 100 arbitrary units for anti-HEL antibodies or 10 arbitrary units for total IgG antibodies.

Diabetes incidence study

Diabetes incidence was monitored daily in female 3A9 TCR:iHEL mice for overt signs of diabetes (wet cage, hunched posture) and every 2 weeks for urine glucose levels using Diastix (Bayer, Toronto, Ontario, Canada) starting at 8 to 12 weeks of age. After two successive positive Diastix tests, overt diabetes is confirmed by blood glucose levels higher than 17 mmol/l. The age of diabetes onset is set at the first detection of elevated urine glucose levels. The mice were sacrificed within 1 week of detection of high blood glucose or when they reached more than 28 weeks of age. At culling, tail DNA was collected to verify the genotype of the mouse. The serum was collected and the pancreas was conserved in formalin for at least 48 h at room temperature before being sent for paraffin inclusion.

Pathway analysis

Genes lists (and MGI ID) from *Idd2* (chromosome 9:29.6–50.3 Mb) and *Idd13* (chromosome 2:114.0–156.1 Mb) were retrieved by the Genes and Markers Query search tool from MGI (Eppig et al. 2015). MGI ID were submitted to DAVID bioinformatics database (Huang et al. 2009a, b). To rescue some unmapped genes (via MGI ID) that did not match with the DAVID database, we sent two lists of unmapped genes to DAVID to get their DAVID ID. MGI and DAVID ID lists were submitted to DAVID and were merged for each locus. *Mus musculus* genome was specified as background. A third list

was built combining all genes from *Idd2* and *Idd13* (*Idd2/13*) loci. All olfactory genes (beginning with “Olfir”) were removed from gene lists as they are expected to have little impact on immunological processes. Olfactory genes represent 21% of genes from *Idd2* locus. For these three gene lists (*Idd2* only, *Idd13* only, *Idd2* and *Idd13* combined), all categories from “disease,” “functional categories,” and “pathways” were selected as well as the subcategories containing “all” from the “gene ontology” category. Functional annotation clustering was performed with default options except for three options: “similarity threshold,” “final group membership,” and “EASE.” They were set to 0.4, 0.6, and 0.05, respectively. Each cluster made by each analysis was named based on the biological processes present in that cluster and compared to the other two analysis results. Highly similar clusters, in the same and/or in different analysis, were grouped under the same biological process. Genes from each biological process produced with the *Idd2/13* genes list were compiled separately and identified as located on chromosome 2 (*Idd13*) or 9 (*Idd2*). DAVID revealed a total of 9 pathways for *Idd2*, 5 for *Idd13*, and 15 for the combined list of *Idd2/13*. One biological process (transferase) present in *Idd2/13* contained only genes from *Idd13* and was excluded from further analysis. The metabolic process was too broad as it comprised almost all of the genes from both loci and this pathway was also discarded for STRING analysis.

STRING analysis

Gene (protein) lists of 13 of the 15 identified biological processes for *Idd2/13* were submitted to STRING analysis individually (Szkarczyk et al. 2015). All associations made by STRING between the input list and their database were manually validated. Only “co-expression,” “experiments,” and “databases” categories were selected for the active prediction methods. Confidence score was set to 0.15 to retrieve text file results and was set to 0.7 to retrieve pathway interactions images. Only links between genes from *Idd2* and *Idd13* loci were selected for further analysis. At least 50% of all links (between genes from the two loci) had to have a confidence score of at least 0.7 to be selected as a final biological process of interest (Table 5). Two different biological processes (sodium transport and peptides) did not show any interaction between genes from *Idd2* and *Idd13* and were excluded from further investigations.

Western blots

Dry pellets of homogenized spleen from B10.BR, NOD.*H2^k*, NOD.*H2^k-Idd2*, NOD.*H2^k-Idd13*, and NOD.*H2^k-Idd2/13* were resuspended in NuPAGE® LDS Sample Buffer (106 mM Tris-HCl, 141 mM Tris Base, 2% lithium dodecyl sulfate, 10% Glycerol, 0.51 mM EDTA, 0.22 mM SERVA

Blue G250, 0.175 mM Phenol Red) and sonicated at 30% intensity for 10 s three times. Protein concentrations were acquired by NanoDrop Microvolume Spectrophotometer. The proteins were loaded on 12% NuPAGE® gels at 200 V. Migrated proteins were transferred to PVDF membranes, blocked with 5% milk and 3% BSA in Tris-buffered saline with 0.1% Tween 20 (TBS-T) for 1 h at room temperature. Separate membranes were incubated overnight at 4 °C with mouse anti- α Tubulin (Abcam, ab7291), rabbit anti-RAD51 (BioAcademia, 70-002), and anti-H2AX (Bethyl, A300-082A) antibodies. Following washes with TBS-T, the membranes were incubated with either anti-rabbit or anti-mouse-Horseradish peroxidase (HRP)-conjugated secondary antibodies for 1 h at room temperature. Chemiluminescence was acquired on an Azure c600 (Azure Biosystems). Quantification and normalization of the protein bands were performed on ImageJ.

Statistical analysis

Statistical significance was determined using one-way ANOVA with Bonferroni post-HOC test for differences between more than two groups and a paired or unpaired Student *t* test was used when testing for significant difference between two groups, as appropriate.

Funding information This work was supported by a grant from the Canadian Diabetes Association (OG-3-13-4018) to SL. SL holds a Senior scholarship and RC holds studentship both from Fonds de recherche du Québec-Santé, and VMD holds a studentship from l'Université de Montréal. MK received a doctoral fellowship from the Cole Foundation. AO is the Canada Research Chair (Tier 2) in Genome Stability and Hematological Malignancies. Work in the AO laboratory was supported by a Transition Grant from the Cole Foundation and an internal Operating Fund from the Sir Mortimer B. Davis Foundation of the Jewish General Hospital.

Compliance with ethical standards

Conflict of interest The authors declare that they have no conflict of interest.

References

- Akkaraju S, Ho WY, Leong D, Canaan K, Davis MM, Goodnow CC (1997) A range of CD4 T cell tolerance: partial inactivation to organ-specific antigen allows nondestructive thyroiditis or insulinitis. *Immunity* 7:255–271
- Anderson MS, Bluestone JA (2005) THE NOD MOUSE: a model of immune dysregulation. *Annu Rev Immunol* 23:447–485
- Anderson MS, Venanzi ES, Klein L, Chen Z, Berzins SP, Turley SJ, von Boehmer H, Bronson R, Dierich A, Benoist C, Mathis D (2002) Projection of an immunological self shadow within the thymus by the aire protein. *Science* 298:1395–1401
- Berti M, Vindigni A (2016) Replication stress: getting back on track. *Nat Struct Mol Biol* 23:103–109
- Bluestone JA, Auchincloss H, Nepom GT, Rotrosen D, St Clair EW, Turka LA (2010a) The immune tolerance network at 10 years: tolerance research at the bedside. *Nat Rev Immunol* 10:797–803
- Bluestone JA, Herold K, Eisenbarth G (2010b) Genetics, pathogenesis and clinical interventions in type 1 diabetes. *Nature* 464:1293–1300
- Boutros R, Lobjois V, Ducommun B (2007) CDC25B involvement in the centrosome duplication cycle and in microtubule nucleation. *Cancer Res* 67:11557–11564
- Bugler B, Schmitt E, Aressy B, Ducommun B (2010) Unscheduled expression of CDC25B in S-phase leads to replicative stress and DNA damage. *Mol Cancer* 9:29
- Chen W, Ford MS, Young KJ, Zhang L (2003) Infusion of in vitro-generated DN T regulatory cells induces permanent cardiac allograft survival in mice. *Transplant Proc* 35:2479–2480
- Collin R, Dugas V, Pelletier AN, Chabot-Roy G, Lesage S (2014) The mouse *idd2* locus is linked to the proportion of immunoregulatory double-negative T cells, a trait associated with autoimmune diabetes resistance. *J Immunol* 193:3503–3512
- Concannon P, Rich SS, Nepom GT (2009) Genetics of type 1A diabetes. *N Engl J Med* 360:1646–1654
- Driver JP, Serreze DV, Chen YG (2011) Mouse models for the study of autoimmune type 1 diabetes: a NOD to similarities and differences to human disease. *Semin Immunopathol* 33:67–87
- Dugas V, Beauchamp C, Chabot-Roy G, Hillhouse EE, Lesage S (2010) Implication of the CD47 pathway in autoimmune diabetes. *J Autoimmun* 35:23–32
- Dugas V, Chabot-Roy G, Beauchamp C, Guimont-Desrochers F, Hillhouse EE, Liston A, Lesage S (2013) Unusual selection and peripheral homeostasis for immunoregulatory CD4⁽⁻⁾ CD8⁽⁻⁾ T cells. *Immunology* 139:129–139
- Dugas V, Liston A, Hillhouse EE, Collin R, Chabot-Roy G, Pelletier AN, Beauchamp C, Hardy K, Lesage S (2014) *Idd13* is involved in determining immunoregulatory DN T-cell number in NOD mice. *Genes Immun* 15:82–87
- Duncan B, Nazarov-Stoica C, Surls J, Kehl M, Bona C, Casares S, Brumeanu TD (2010) Double negative (CD3⁺ 4⁻ 8⁻) TCR alphabeta splenic cells from young NOD mice provide long-lasting protection against type 1 diabetes. *PLoS One* 5:e11427
- Elledge SJ (1996) Cell cycle checkpoints: preventing an identity crisis. *Science* 274:1664–1672
- Eppig JT, Blake JA, Bult CJ, Kadin JA, Richardson JE (2015) The Mouse Genome Database (MGD): facilitating mouse as a model for human biology and disease. *Nucleic Acids Res* 43:D726–D736
- Ford MS, Chen W, Wong S, Li C, Vanama R, Elford AR, Asa SL, Ohashi PS, Zhang L (2007) Peptide-activated double-negative T cells can prevent autoimmune type-1 diabetes development. *Eur J Immunol* 37:2234–2241
- Garner-Hamrick PA, Fisher C (1998) Antisense phosphorothioate oligonucleotides specifically down-regulate *cdc25B* causing S-phase delay and persistent antiproliferative effects. *Int J Cancer* 76:720–728
- Genin A, Desir J, Lambert N, Biervliet M, Van Der Aa N, Pierquin G, Killian A, Tosi M, Urbina M, Lefort A, Libert F, Pirson I, Abramowicz M (2012) Kinetochore KMN network gene *CASC5* mutated in primary microcephaly. *Hum Mol Genet* 21:5306–5317
- Ghosh S, Palmer SM, Rodrigues NR, Cordell HJ, Heame CM, Cornell RJ, Prins JB, McShane P, Lathrop GM, Peterson LB, Wicker LS, Todd JA (1993) Polygenic control of autoimmune diabetes in nonobese diabetic mice. *Nat Genet* 4:404–409
- He KM, Ma Y, Wang S, Min WP, Zhong R, Jevnikar A, Zhang ZX (2007) Donor double-negative Treg promote allogeneic mixed chimerism and tolerance. *Eur J Immunol* 37:3455–3466
- Hillhouse EE, Beauchamp C, Chabot-Roy G, Dugas V, Lesage S (2010) Interleukin-10 limits the expansion of immunoregulatory CD4⁻CD8⁻ T cells in autoimmune-prone non-obese diabetic mice. *Immunol Cell Biol* 88:771–780

- Hillhouse EE, Collin R, Chabot-Roy G, Guyon MJ, Tessier N, Boulay M, Liscourt P, Lesage S (2013) Nearby construction impedes the progression to overt autoimmune diabetes in NOD mice. *J Diabetes Res* 2013:620313
- Hillhouse EE, Liston A, Collin R, Desautels E, Goodnow CC, Lesage S (2016) TCR transgenic mice reveal the impact of type 1 diabetes loci on early and late disease checkpoints. *Immunol Cell Biol* 94:709–713
- Ho WY, Cooke MP, Goodnow CC, Davis MM (1994) Resting and anergic B cells are defective in CD28-dependent costimulation of naive CD4+ T cells. *J Exp Med* 179:1539–1549
- Huang d W, Sherman BT, Lempicki RA (2009a) Bioinformatics enrichment tools: paths toward the comprehensive functional analysis of large gene lists. *Nucleic Acids Res* 37:1–13
- Huang d W, Sherman BT, Lempicki RA (2009b) Systematic and integrative analysis of large gene lists using DAVID bioinformatics resources. *Nat Protoc* 4:44–57
- Kramer A, Mailand N, Lukas C, Syljuasen RG, Wilkinson CJ, Nigg EA, Bartek J, Lukas J (2004) Centrosome-associated Chk1 prevents premature activation of cyclin-B-Cdk1 kinase. *Nat Cell Biol* 6:884–891
- Lam MH, Liu Q, Elledge SJ, Rosen JM (2004) Chk1 is haploinsufficient for multiple functions critical to tumor suppression. *Cancer Cell* 6:45–59
- Lammer C, Wagerer S, Saffrich R, Mertens D, Ansoerge W, Hoffmann I (1998) The cdc25B phosphatase is essential for the G2/M phase transition in human cells. *J Cell Sci* 111(Pt 16):2445–2453
- Lang J, Bellgrau D (2004) Animal models of type 1 diabetes: genetics and immunological function. *Adv Exp Med Biol* 552:91–116
- Lesage S, Hartley SB, Akkaraju S, Wilson J, Townsend M, Goodnow CC (2002) Failure to censor forbidden clones of CD4 T cells in autoimmune diabetes. *J Exp Med* 196:1175–1188
- Liston A, Hardy K, Pittelkow Y, Wilson SR, Makaroff LE, Fahrner AM, Goodnow CC (2007) Impairment of organ-specific T cell negative selection by diabetes susceptibility genes: genomic analysis by mRNA profiling. *Genome Biol* 8:R12
- Liston A, Lesage S, Gray DHD, O'Keefe CL, Reilly LA, Strasser a, Fahrner AM, Boyd RL, Wilson J, Baxter AG, Gallo EM. (2004) Generalized resistance to thymic deletion in the NOD MouseA polygenic trait characterized by defective induction of Bim. *Immunity* 21:817–830
- Lutzmann M, Grey C, Traver S, Ganier O, Maya-Mendoza A, Ranisavljevic N, Bernex F, Nishiyama A, Montel N, Gavois E, Forichon L, de Massy B, Mechali M (2012) MCM8- and MCM9-deficient mice reveal gametogenesis defects and genome instability due to impaired homologous recombination. *Mol Cell* 47:523–534
- Lyons PA, Hancock WW, Denny P, Lord CJ, Hill NJ, Armitage N, Siegmund T, Todd JA, Phillips MS, Hess JF, Chen SL, Fischer PA, Peterson LB, Wicker LS (2000) The NOD Idd9 genetic interval influences the pathogenicity of insulinitis and contains molecular variants of Cd30, Tnfr2, and Cd137. *Immunity* 13:107–115
- Ma Y, He KM, Garcia B, Min W, Jevnikar A, Zhang ZX (2008) Adoptive transfer of double negative T regulatory cells induces B-cell death in vivo and alters rejection pattern of rat-to-mouse heart transplantation. *Xenotransplantation* 15:56–63
- Maiorano D, Cuvier O, Danis E, Mechali M (2005) MCM8 is an MCM2-7-related protein that functions as a DNA helicase during replication elongation and not initiation. *Cell* 120:315–328
- McAleer MA, Reifsnnyder P, Palmer SM, Prochazka M, Love JM, Copeman JB, Powell EE, Rodrigues NR, Prins JB, Serreze DV et al (1995) Crosses of NOD mice with the related NON strain. A polygenic model for IDDM. *Diabetes* 44:1186–1195
- McIver Z, Serio B, Dunbar A, O'Keefe CL, Powers J, Wlodarski M, Jin T, Sobels R, Bolwell B, Maciejewski JP (2008) Double-negative regulatory T cells induce allotolerance when expanded after allogeneic haematopoietic stem cell transplantation. *Br J Haematol* 141:170–178
- Park J, Long DT, Lee KY, Abbas T, Shibata E, Negishi M, Luo Y, Schimenti JC, Gambus A, Walter JC, Dutta A (2013) The MCM8-MCM9 complex promotes RAD51 recruitment at DNA damage sites to facilitate homologous recombination. *Mol Cell Biol* 33:1632–1644
- Patil M, Pabla N, Dong Z (2013) Checkpoint kinase 1 in DNA damage response and cell cycle regulation. *Cell Mol Life Sci* 70(21):4009–4021
- Pearce RB, Formby B, Healy K, Peterson CM (1995) Association of an androgen-responsive T cell phenotype with murine diabetes and Idd2. *Autoimmunity* 20:247–258
- Pelletier AN, Lesage S (2013) The Idd13 congenic interval defines the number of merocytic dendritic cells, a novel trait associated with autoimmune diabetes susceptibility. *J Autoimmun* 43:70–77
- Petermann E, Woodcock M, Helleday T (2010) Chk1 promotes replication fork progression by controlling replication initiation. *Proc Natl Acad Sci U S A* 107:16090–16095
- Peterson DA, DiPaolo RJ, Kanagawa O, Unanue ER (1999) Quantitative analysis of the T cell repertoire that escapes negative selection. *Immunity* 11:453–462
- Prochazka M, Leiter EH, Serreze DV, Coleman DL (1987) Three recessive loci required for insulin-dependent diabetes in nonobese diabetic mice. *Science* 237:286–289
- Ratiu JJ, Racine JJ, Hasham MG, Wang Q, Branca JA, Chapman HD, Zhu J, Donghia N, Philip V, Schott WH, Wasserfall C, Atkinson MA, Mills KD, Leeth CM, Serreze DV (2017) Genetic and small molecule disruption of the AID/RAD51 axis similarly protects nonobese diabetic mice from type 1 diabetes through expansion of regulatory B lymphocytes. *J Immunol* 198:4255–4267
- Serreze DV, Bridgett M, Chapman HD, Chen E, Richard SD, Leiter EH (1998) Subcongenic analysis of the Idd13 locus in NOD/Lt mice: evidence for several susceptibility genes including a possible diabetogenic role for beta 2-microglobulin. *J Immunol* 160:1472–1478
- Serreze DV, Prochazka M, Reifsnnyder PC, Bridgett MM, Leiter EH (1994) Use of recombinant congenic and congenic strains of NOD mice to identify a new insulin-dependent diabetes resistance gene. *J Exp Med* 180:1553–1558
- Sorensen CS, Hansen LT, Dziegielewski J, Syljuasen RG, Lundin C, Bartek J, Helleday T (2005) The cell-cycle checkpoint kinase Chk1 is required for mammalian homologous recombination repair. *Nat Cell Biol* 7:195–201
- Szklarczyk D, Franceschini A, Wyder S, Forslund K, Heller D, Huerta-Cepas J, Simonovic M, Roth A, Santos A, Tsafou KP, Kuhn M, Bork P, Jensen LJ, von Mering C (2015) STRING v10: protein-protein interaction networks, integrated over the tree of life. *Nucleic Acids Res* 43:D447–D452
- Taylor SS, McKeon F (1997) Kinetochores localization of murine Bub1 is required for normal mitotic timing and checkpoint response to spindle damage. *Cell* 89:727–735
- Vallee RB, Varma D, Dujardin DL (2006) ZW10 function in mitotic checkpoint control, dynein targeting and membrane trafficking: is dynein the unifying theme? *Cell Cycle* 5:2447–2451
- Varma D, Dujardin DL, Stehman SA, Vallee RB (2006) Role of the kinetochores/cell cycle checkpoint protein ZW10 in interphase cytoplasmic dynein function. *J Cell Biol* 172:655–662
- Willet MA, Flores RR, Wang Y, Yi Z, Kroger CJ, Mathews CE, Earp HS, Matsushima G, Wang B, Tisch R (2009) MerTK regulates thymic selection of autoreactive T cells. *Proc Natl Acad Sci U S A* 106:4810–4815
- Wicker LS, Clark J, Fraser HI, Gamer VE, Gonzalez-Munoz A, Healy B, Howlett S, Hunter K, Rainbow D, Rosa RL, Smink LJ, Todd JA, Peterson LB (2005) Type 1 diabetes genes and pathways shared by humans and NOD mice. *J Autoimmun* 25(Suppl):29–33
- Wicker LS, Todd JA, Peterson LB (1995) Genetic control of autoimmune diabetes in the NOD mouse. *Annu Rev Immunol* 13:179–200

- Young KJ, DuTemple B, Phillips MJ, Zhang L (2003) Inhibition of graft-versus-host disease by double-negative regulatory T cells. *J Immunol* 171:134–141
- Young KJ, Yang L, Phillips MJ, Zhang L (2002) Donor-lymphocyte infusion induces transplantation tolerance by activating systemic and graft-infiltrating double-negative regulatory T cells. *Blood* 100:3408–3414
- Zhang D, Zhang W, Ng TW, Wang Y, Liu Q, Gorantla V, Lakkis F, Zheng XX (2011) Adoptive cell therapy using antigen-specific CD4⁺CD8⁻ T regulatory cells to prevent autoimmune diabetes and promote islet allograft survival in NOD mice. *Diabetologia* 54:2082–2092
- Zhang ZX, Ma Y, Wang H, Arp J, Jiang J, Huang X, He KM, Garcia B, Madrenas J, Zhong R (2006) Double-negative T cells, activated by xenoantigen, lyse autologous B and T cells using a perforin/granzyme-dependent, fas-fas ligand-independent pathway. *J Immunol* 177:6920–6929
- Zhang ZX, Yang L, Young KJ, DuTemple B, Zhang L (2000) Identification of a previously unknown antigen-specific regulatory T cell and its mechanism of suppression. *Nat Med* 6:782–789
- Zucchelli S, Holler P, Yamagata T, Roy M, Benoist C, Mathis D (2005) Defective central tolerance induction in NOD mice: genomics and genetics. *Immunity* 22:385–396